Cell Mol Neurobiol (2017) 37:453–460
DOI 10.1007/s10571-016-0378-8

ORIGINAL RESEARCH

Thiamine Deficiency Increases Ca^{2+} Current and $Ca_V1.2$ L-type Ca^{2+} Channel Levels in Cerebellum Granular Neurons

Daniel C. Moreira-Lobo[1] · Jader S. Cruz[1] · Flavia R. Silva[1] · Fabíola M. Ribeiro[1] · Christopher Kushmerick[2] · Fernando A. Oliveira[3]

Received: 19 November 2015 / Accepted: 22 April 2016 / Published online: 2 May 2016

Abstract Thiamine (vitamin B1) is co-factor for three pivotal enzymes for glycolytic metabolism: pyruvate dehydrogenase, α-ketoglutarate dehydrogenase, and transketolase. Thiamine deficiency leads to neurodegeneration of several brain regions, especially the cerebellum. In addition, several neurodegenerative diseases are associated with impairments of glycolytic metabolism, including Alzheimer's disease. Therefore, understanding the link between dysfunction of the glycolytic pathway and neuronal death will be an important step to comprehend the mechanism and progression of neuronal degeneration as well as the development of new treatment for neurodegenerative states. Here, using an in vitro model to study the effects of thiamine deficiency on cerebellum granule neurons, we show an increase in Ca^{2+} current density and $Ca_V1.2$ expression. These results indicate a link between alterations in glycolytic metabolism and changes to Ca^{2+} dynamics, two factors that have been implicated in neurodegeneration.

Keywords Ca^{2+} current · Thiamine · Cerebellum · Granular neuron · Neurodegeneration

✉ Jader S. Cruz
jcruz@icb.ufmg.br

✉ Fernando A. Oliveira
oliveira.fernando@ufabc.edu.br

[1] Department of Biochemistry and Immunology, Institute of Biological Sciences, Universidade Federal de Minas Gerais, Avenida Antônio Carlos, 6627, Bloco K4, Sala #167, Belo Horizonte, MG CEP 31270-901, Brazil

[2] Department of Physiology and Biophysics, Institute of Biological Sciences, Universidade Federal de Minas Gerais, Avenida Antônio Carlos, 6627, Belo Horizonte MG, CEP 31270-901, Brazil

[3] Center for Mathematics, Computing and Cognition (CMCC), Universidade Federal do ABC – UFABC, Rua Arcturus, 03 – Jardim Antares, Bloco Delta; 2° Andar; Sala: 248, São Bernardo do Campo, SP CEP 09606-070, Brazil

Introduction

Thiamine is a co-factor for pyruvate dehydrogenase, α-ketoglutarate dehydrogenase, and transketolase. Although essential for the correct functioning of the Krebs cycle, no animals synthesize thiamine and it must be obtained from the diet. Skeletal muscle, heart, kidney, and liver can store thiamine; however, in humans, these stores are depleted in weeks under a diet deficient in thiamine, since the thiamine biological half-life is between 9 and 18 days (Pácal et al. 2014). The consequences of thiamine deficiency include beriberi and Wernicke encephalopathy, a neurodegenerative disease that causes loss of neurons in the central nervous system, mainly in the cerebellum (Butterworth 1993; Mulholland 2006; Pannunzio et al. 2000; Troncoso et al. 1981). Epidemiological evidence suggests that Wernicke encephalopathy is an under diagnosed disease, with an especially high prevalence among alcoholics and other undernourished individuals (Day and del Campo 2014; Galvin et al. 2010).

The brain is more vulnerable to thiamine deficiency than other tissues. Likely, this is due to the very high energy demand of the brain that makes it particularly susceptible to any impairment of energy metabolism. However, the link between thiamine deficiency and neuronal degeneration in the brain is still unclear. Several hypotheses have been raised, including increased oxidative stress, mitochondrial dysfunction, and activation of caspase

3-dependent apoptotic pathways (Chornyy et al. 2007; Kang et al. 2010; Yadav et al. 2010). One of the main triggers may be an overload of Ca^{2+}. Previous studies demonstrated changes to Ca^{2+} permeable AMPA receptors leading to increased basal Ca^{2+} levels and Ca^{2+} dynamics when cultured cortical neurons were maintained in the presence of an inhibitor of the thiamine transporter (Lee et al. 2010).

Furthermore, the thiamine deficiency is a well-established model for the condition of oxidative stress (Wang et al. 2007) and knowing that NO may modulate Ca^{2+} channel expression in cerebellum granular neurons (Kim et al. 2004); we hypothesized that thiamine deficiency could modify $Ca_V1.2$ levels in cerebellum granular neurons. In addition, $Ca_V1.2$ blockers are easy to use for future in vitro and in vivo tests. However, the possibility of altered Ca^{2+} handling in cerebellum granular neurons during thiamine deficiency is currently unknown. Previously, we developed an in vitro preparation to study thiamine deficiency by maintaining cerebellum granular neurons on culture with thiamine-deficient media and studied effects on ion channels and electrophysiological parameters (Cruz et al. 2012; Oliveira et al. 2007). In the present paper, we used this preparation to measure the effects of thiamine deficiency on whole-cell Ca^{2+} currents and $Ca_V1.2$ protein levels in cerebellum granular neurons.

Materials and Methods

Cell Culture

The investigation was conducted according to the Guidelines for the Care and Use of Laboratory Animals published by the National Institutes of Health (USA) and the Institutional Ethics Committee for Animal Experimentation (CEUA-UFMG, protocol number 4/2010). Cells were cultured as previously described (Oliveira et al. 2007; Cruz et al. 2012). Unless stated otherwise, reagents were from Sigma-Aldrich. Briefly, newborn Wistar rats were killed by decapitation. Cerebellum were dissected and placed in Ca^{2+}-free Hanks solution (0 °C) of the following composition (in mM): NaCl 136.9, KCl 5.3, KH_2PO_4 0.44, Na_2HPO_4 0.33, $NaHCO_3$ 4, and Glucose 5.5, pH 7.4 (adjusted with NaOH). Penicillin and streptomycin were added by including 1 % of an antibiotic stock solution containing 10.000 units/ml penicillin and 10.000 mg/ml streptomycin. The tissue was cut in small pieces (1–2 mm) and digested with trypsin (2.5 mg/ml) for 5 min. The trypsin solution was removed and the cerebellum fragments were washed three times in DMEM supplemented with 10 % fetal bovine serum (Cripion Biotechnology, Campinas, Brazil) and 1 % antibiotic solution. Cells were mechanically dissociated by passing the tissue fragments through three glass pipettes with decreasing tip diameters. Dissociated cells were centrifuged for one minute at 1000 RPM and then resuspended in thiamine (−) or thiamine (+) [0.004 g/l] DMEM supplemented with 10 % fetal bovine serum and 1 % antibiotics as above. The cells were plated at a density of 2×10^6 cells/cm^2 onto poly-D-lysine-coated glass coverslips (18 × 18 mm) and maintained at 37 °C, 5 % CO_2 for 1 h. After this time, the culture medium was exchanged and 0.4 µg/ml cytosine arabinoside (Ara-C) was added to prevent glial proliferation. Cells were maintained in an incubator at 37 °C in an atmosphere of 5 % CO_2. Every three days, 800 µl of medium was removed from each dish and 1 ml of fresh medium (with Ara-C) was added. Cells were maintained in either thiamine (−) or thiamine (+) culture medium for 7–8 days and then used for Western blot or patch-clamp experiments.

Electrophysiological Recordings

Macroscopic currents were recorded at room temperature (24–28 °C) with the whole-cell configuration of the patch-clamp technique (Hamill et al. 1981) using an EPC-9 amplifier (HEKA Instruments, Germany) connected to a PC computer. The holding potential was −80 mV unless otherwise stated. Patch-clamp pipettes were made of soft glass capillaries (Perfecta, Brazil) using a vertical 2-stage puller (Narishige, Japan) and were backfilled with an internal solution containing (in mM): CsCl 120; $MgCl_2$ 1; EGTA 10; HEPES 10; Mg-ATP 2; and pH 7.2 (adjusted with CsOH). Open tip patch pipette resistances were 3–5 MΩ. The protocols were generated and data acquired with Pulse software (HEKA Instruments, Germany) at an acquisition frequency of 20 kHz and low-pass filtered at a cut-off frequency of 2.9 kHz. Series resistance was less than 15 MΩ and compensated by 75 %. Leak subtraction was performed online using a P/4 protocol. Leak current was <25 pA. Access resistance was verified before and after each recording and those cells that showed more than 20 % change in the access resistance were discarded from the analysis. Junction potentials were not corrected.

To obtain giga-ohm seal in neurons, we used an external solution containing (in mM): NaCl 140; KCl 5.4; $CaCl_2$ 1.8; $MgCl_2$ 0.5; NaH_2PO_4 0.33; Glucose 11; HEPES 5; and pH 7.4 (adjusted with NaOH). After achieving whole-cell configuration, the cell was superfused at 6 µl/s with an external solution containing (in mM): TEA-Cl 130; $MgCl_2$ 2; $BaCl_2$ 10; HEPES 10; Glucose 10; and pH 7.2 (adjusted with TEA-OH). The external and pipette solutions were designed to completely suppress Na^+ and K^+ currents, leaving only the Ba^{2+} currents (I_{Ba}) through voltage-dependent Ca^{2+} channels.

Stimulation Protocols

To record Ba^{2+} currents, two protocols were applied: slow ramps and square wave pulse protocols. In both of these protocols, cells were held at −80 mV. Ramps were from −80 mV to +50 mV over 100 ms. The ramp protocol was repeated 12 times, once every 15 s, starting immediately after achieving whole-cell. Following the series of ramps protocols, we applied square wave protocol consisted of test pulses of 70 ms duration ranging from −50 to 50 mV in 5 mV steps, followed by a test pulse to 0 mV to measure current inactivation. For I–V and G–V analysis, we only included cells that exhibited less than 10 % rundown from the beginning to end of the ramp protocols. Between step depolarizations, cells were held for 15 s at −80 mV to allow full recovery from inactivation.

Immunoblotting

Cerebellum neuronal cultures were maintained in thiamine (+) or thiamine (−) culture media for 7 days and then lysed in Triton buffer (in mM: NaCl 150, Tris–HCl 50, 1 % Triton X-100, and pH 7.4) containing protease inhibitors (1 mM AEBSF and 10 μg/ml of both leupeptin and aprotinin). 100 μg of total cellular protein for each sample were subjected to SDS-PAGE, followed by electroblotting onto nitrocellulose membranes. Membranes were blocked with 10 % non-fat milk in wash buffer (in mM) NaCl 150, Tris–HCl 10, 0.05 % Tween-20, and pH 7.4 for 1 h and then incubated with either rabbit anti-$Ca_V1.2$ (1:200; Millipore #MAB13170) or rabbit anti-actin (1:1000, Sigma-Aldrich) antibodies in wash buffer containing 3 % non-fat milk for 2 h at room temperature (24–26 °C). Membranes were rinsed three times with wash buffer and then incubated with secondary peroxidase-conjugated anti-rabbit IgG antibody diluted 1:5000 in wash buffer containing 3 % non-fat milk for 1 h. Membranes were rinsed three times with wash buffer and incubated with ECL Western blotting detection reagents.

Modeling

Simulations were performed in the Neuron modeling environment (Hines and Carnevale 1997). The original cerebellum granular neuron model was published by D'Angelo et al. (2001). Recently, we described how this model could be modified to reflect the effects of thiamine deficiency on A-type K^+ currents (for details, Cruz et al. 2012). Here, we extend our modifications of the model to account for the 50 % increase in HVA Ca^{2+} currents. We modeled two situations, normal HVA Ca^{2+} current density (control) and 1.5 times the normal density of HVA Ca^{2+} current, as recorded experimentally in thiamine-deficient neurons. As we described in detail previously (Cruz et al. 2012), the functional effects on excitability can be probed using simulated synaptic stimulation. We examined two aspects of excitability: refractory periods (defined here as an increase in threshold for a second EPSC following a previous suprathreshold EPSC) and temporal summation of EPSPs (defined here as a decrease in threshold for a second EPSC following a previous subthreshold EPSC). In this approach, the model cell was stimulated with pairs of synaptic inputs (conductances) that were based on the kinetics previously describe for mossy fiber inputs to granular neurons (Sola et al. 2004). The interval between pairs of synaptic conductance was varied systematically from 1.5 to 160 ms. At each time interval, refractoriness and temporal summation were measured. To measure refractoriness, the amplitude of the first synaptic input was set to 1.5 times threshold (i.e., 1.5 times the minimum synaptic input necessary to generate an action potential) and then threshold was determined for the second synaptic input as the minimum synaptic conductance needed to generate an action potential. To measure temporal summation, the amplitude of the first synaptic input was set to 90 % of threshold and then threshold for the second synaptic input was determined as for refractoriness. In both cases, the threshold synaptic conductance of the second stimulus was measured as a function of the interpulse interval and normalized relative to its values for infinitely long intervals.

Analysis

Electrophysiology Data

Currents were analyzed using routines developed in the Python and C++ programming languages written by DCML. Ca^{2+} current amplitudes were defined as the maximal inward current during ramp or step depolarization protocols. Ca^{2+} conductance was determined by fitting Eq. 1 to current–voltage (I–V) data.

$$i(v) = g_{\max} \times (V - E_{Ca}) \times \left(1 + e^{\frac{-(v-v_a)}{k_a}}\right)^{-1}, \quad (1)$$

where $g_{\max}$ is the maximum Ca^{2+} conductance, E_{Ca} is the Ca^{2+} current reversal potential, and ($\sim$+50 mV) determined individually for each cell as the intersection between the linear rising phase of the I–V relationship and the v axis. v is the test potential, v_a is the voltage required for half-maximal activation, and k_a is the steepness of the voltage dependence.

Conductance (g) as a function of membrane potential (v) was calculated according to Eq. 2:

$$g(v) = i/(v - E_{Ca}), \quad (2)$$

where E_{Ca} is the Ca^{2+} current reversal potential (see above). The derived G–V data was then used to adjust

Eq. 3 to determine g_{max}, the half activation potential (v_a), and the steepness of the voltage dependence (k).

$$g(v) = g_{max}\left(1 + e^{\frac{-(v-v_a)}{k_a}}\right)^{-1}. \quad (3)$$

To obtain the voltage for half inactivation, the normalized current was fitted by a modified Boltzmann equation (Eq. 4):

$$i(v) = (1-p)/\left(1 + e^{\frac{(v-v_i)}{k_i}}\right) + p, \quad (4)$$

where, i is the current at the normalized test pulse, p is the fraction of the current that inactivated, v is the voltage of the applied pre-pulse, v_i is the half inactivation potential, and k_i is the steepness of the voltage dependence.

Immunoblotting Analysis

Non-saturated immunoreactive $Ca_V1.2$ and actin bands were quantified by scanning densitometry from total cellular homogenate protein content of each sample. Immunoband intensity was calculated using ImageJ software (NIH), and the intensity of the pixels of $Ca_V1.2$ band was normalized by the intensity of pixels of actin band and reported as percentage.

Statistical Tests

Ca^{2+} current I–V relationship are based on data from at least 5 independent cell cultures. Data are expressed as the mean ± SEM. Statistical testes were done using SigmaPlot 11.0 (Systat Software, Inc). Probability values of $p < 0.05$ were considered to be statistically significant.

Results

To determine the consequences of thiamine deficiency on voltage gated Ca^{2+} channels, we performed whole-cell voltage clamp experiments using Ba^{2+} as the charge carrier under conditions that isolate Ca^{2+} channel current. During ramp protocols, peak current in thiamine-deficient cells was significantly greater than in controls [Thiamine (+): −64.5 ± 3.13 pA/pF, $n = 21$; Thiamine (−): −94.2 ± 7.65 pA/pF, $n = 15$; data not shown]. To study the I–V relationship in more detail, we applied step depolarizations ranging from −50 to 50 mV. As shown in Fig. 1, thiamine deficiency had two marked effects on Ca^{2+} channel currents: an increase in peak current density and a positive shift in the voltage dependence of activation. When measured during a step depolarization to 0 mV (Fig. 1a, b), Ca^{2+} currents were −62.7 ± 11.6 pA/pF in control cells and −103 ± 11.6 pA/pF in thiamine-deficient cells [$n = 5$ for thiamine (+) and $n = 7$ for thiamine (−)]. To determine the increase in conductance, we adjusted Eq. 1 (see "Materials and Methods") to the I–V data (curves in Fig. 1b). Based on the best-

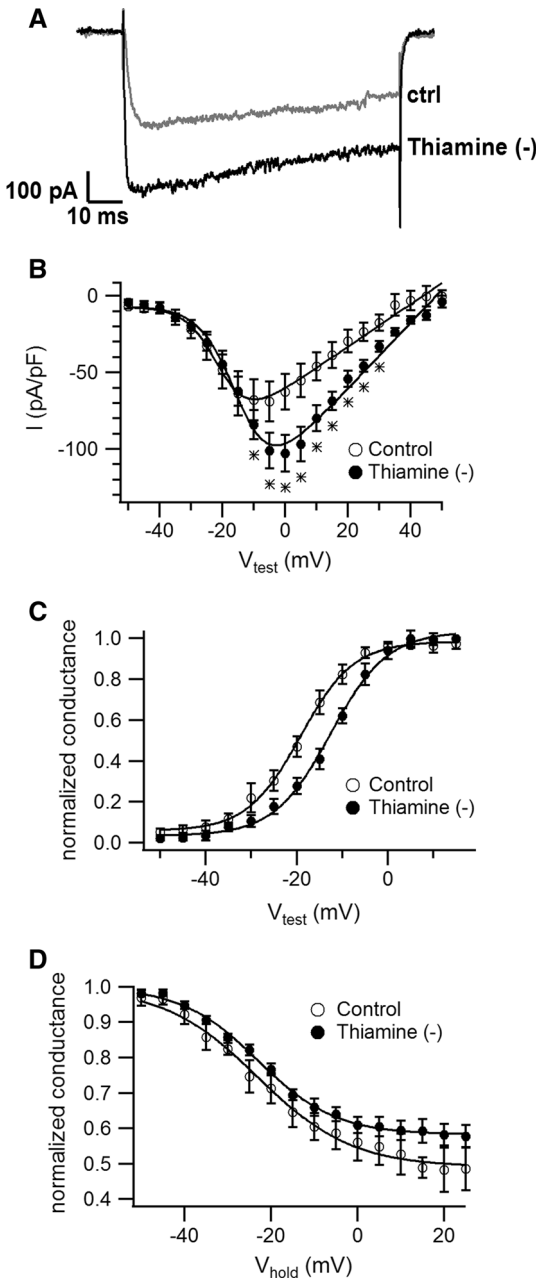

Fig. 1 Thiamine deficiency increases Ca^{2+} current density and shifts the voltage dependence for activation in cerebellum granular neurons. **a** Representative current traces recorded in response to 0 mV depolarization in thiamine (+) (Ctrl; *gray line*) and thiamine (−) (*black line*) conditions. **b** I–V relationships of Ca^{2+} channel current (measured using Ba^{2+} as charge carrier). *Curves* represent the best fit of Eq. 1 (see "Materials and Methods" section) to the data [$n = 5$ for thiamine (+) and $n = 7$ for thiamine (−)]. **c** Normalized G–V relationships obtained from the data in (**b**). *Curves* represent the best fit of Eq. 2 (see "Materials and Methods" section) to the data. **d** Steady-state inactivation. *Curves* represent the best-fit to Eq. 3 (see "Materials and Methods" section), $^*p < 0.05$

fit parameters, Ca^{2+} channel conductance was increased 55 % by thiamine deficiency [g_{max} = 1.39 nS/pF in thiamine (+) vs. 2.15 nS/pF in thiamine (−)].

To quantify the effects of thiamine deficiency on the voltage dependence of activation, we converted the I–V data shown in Fig. 1b to normalized G–V by dividing the amplitude of the measured current by the driving force based on the Ca^{2+} current reversal potential and then normalizing to the largest conductance value (Fig. 1c). By fitting Eq. 3 (see "Materials and Methods" section) to these data, we determined that thiamine deficiency caused a positive shift of 6.6 mV in the voltage required for half-maximal activation [v_a = −19.2 mV in thiamine (+) cells vs. −12.6 mV in thiamine (−) cells]. In contrast, thiamine deficiency did not modify the steepness of the G–V relationship [k_a = 5.8 mV in thiamine (+) cells vs. 6.2 mV in thiamine (−) cells].

To determine if thiamine deficiency altered the voltage dependence of steady-state inactivation, we measured peak Ca^{2+} channel current available after holding the cell for 70 ms at depolarized potentials (Fig. 1d). We observed no significant difference in the potential for half inactivation [v_i = –23.0 mV in thiamine (+) cells vs. −22.9 in thiamine (−) cells].

To estimate the amount of L-type Ca^{2+} channel protein, immunoblotting was performed on cerebellum granular neurons under thiamine (+) and thiamine (−) conditions. Figure 2 shows $Ca_V1.2$ L-type Ca^{2+} channel protein is increased in neurons maintained in thiamine (−) conditions [$Ca_V1.2$/Actin = 0.29 ± 0.02 in thiamine (+) cells vs. 1.08 ± 0.18 in thiamine (−) cells], a 2.7-fold increase.

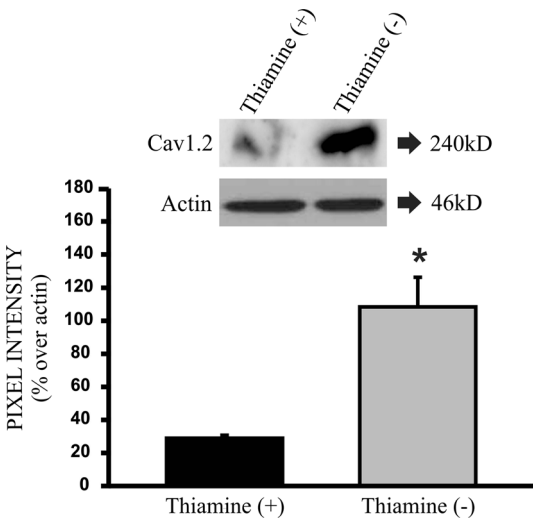

Fig. 2 Immunoblotting for L-type Ca^{2+} channel in cerebellum granular neurons (CGN). CGN cultures were maintained in thiamine (−) [n = 6] or thiamine (+) [n = 6] conditions and then lysed to quantify L-type Ca^{2+} channels using anti-$Ca_V1.2$ antibody (see "Materials and Methods" section). *$p < 0.05$

Cerebellum granular neurons receive synaptic inputs from mossy fibers, and temporal summation of mossy fiber EPSPs is required to bring the granule neuron to threshold (Chadderton et al. 2014). To determine the impact of increased Ca^{2+} channel current on granular neurons firing properties, we modified an existing biophysical model and simulated action potential firing evoked by synaptic stimulation. The biophysical model was based on one published by D'Angelo et al. (2001) and modified to include the observed effects of thiamine deficiency on A-type K^+-currents (Cruz et al. 2012) and HVA Ca^{2+} currents (this study). The model cell was stimulated with synaptic conductance based on fast mossy fiber excitatory post-synaptic currents (Sola et al. 2004). We examined two aspects of excitability: refractory periods (an increase in threshold for a second EPSC following a previous suprathreshold EPSC) and temporal summation (a decrease in threshold for a second EPSC following a previous subthreshold EPSC). These two parameters were determined as a function of the interval between paired stimuli (Paired-pulse interval, Fig. 3). As previously reported (Cruz et al. 2012), the model predicts decreased refractoriness when the effect of thiamine deficiency on A-type K^+ current was included (Fig. 3a, black vs. gray lines). The model predicts little additional effect of increased HVA Ca^{2+} current (Fig. 3a, solid vs. dashed lines). The major effect of increased Ca^{2+} current was a small increase in the absolute refractory period (Fig. 3a, rightward shift in the position of the symbol). As shown in Fig. 3b, increased HVA Ca^{2+} current had essentially no effect on temporal summation, presumably because the first subthreshold EPSC does not significantly activate these channels.

Discussion

In previous studies, we have reported changes to voltage gated channels caused by thiamine deficiency (Cruz et al. 2012; Oliveira et al. 2007). In this paper, we show that thiamine deficiency causes an increase of HVA Ca^{2+} protein levels of HVA Ca^{2+} channel and increased the size of Ca^{2+} currents in cerebellum granular neurons. These data imply a larger influx of Ca^{2+} during each action potential and could result in Ca^{2+} overload. Abnormally high Ca^{2+} entry in neurons has been associated with neurodegenerative conditions (Tymianski et al. 1993; Szydlowska and Tymianski 2010; Mattson 2007) and learning and memory impairments (Kawamoto et al. 2012; Oh et al. 2010; Veng et al. 2003). Several studies have shown that intracellular Ca^{2+} deregulation participates in important pathological processes in Alzheimer's disease (AD). In particular, β-amyloid accumulation may induce intracellular Ca^{2+} enhancements, leading to neuronal cell

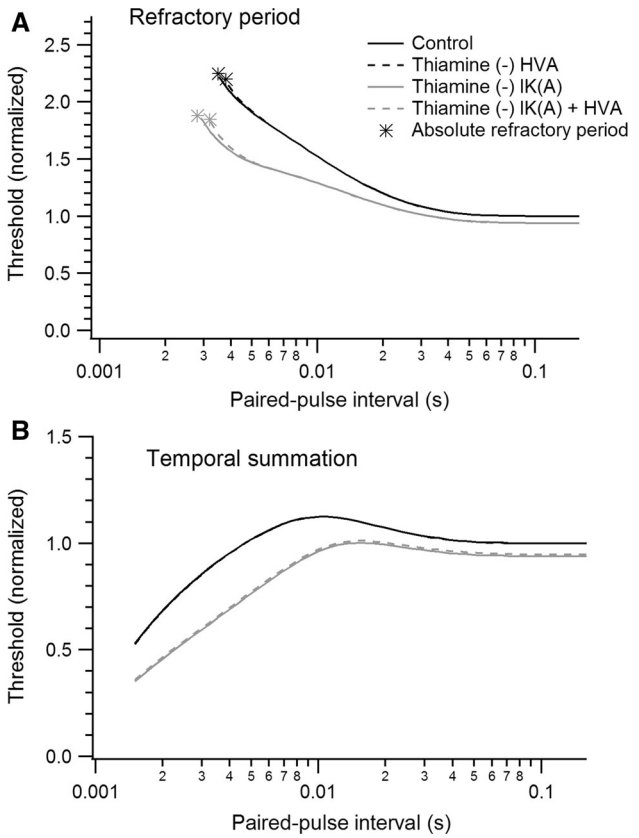

Fig. 3 Computational analysis of the effects of HVA Ca^{2+} current conductance on refractory periods and temporal summation. **a** Refractory periods. The model neuron was stimulated with pairs of synaptic inputs with intervals ranging from 1.5 to 160 ms. The conductance of the first synaptic input was set to 1.5 times action potential (AP) threshold, and the threshold of the second synaptic input to generate an action potential was measured as a function of paired-pulse interval. The symbol indicates the absolute refractory period. *Black lines* represent control thiamine (+) K^+ currents, *gray lines* represent modified A-type K^+ current as reported in Cruz et al. (2012). *Solid lines* represent control Thiamine (+) HVA Ca^{2+} currents, *broken lines* represent Thiamine (−) modified HVA Ca^{2+} currents. **b** Temporal summation. Threshold of a second synaptic conductance was measured when the first synaptic conductance was set to 0.9 times AP threshold. Same color code as for (**a**). For all cases, thresholds are normalized the control values (*Black solid lines*) at the longest interval

dysfunction and death (Davidson et al. 1994; Kim and Rhim 2011; MacManus et al. 2000; Ueda et al. 1997; Gleichmann and Mattson 2011).

Cerebellum granular neurons express several different types of Ca^{2+} channels. In a previous study using very similar experimental conditions, Randall and Tsien (1995) distinguished five pharmacologically distinct HVA Ca^{2+} channel currents in rat cerebellum granular neurons: nimodipine-sensitive L-type Ca^{2+} current, ω-conotoxin-GIVA-sensitive N-type Ca^{2+} current, ω-Agatoxin-IVA-sensitive P- and Q-type Ca^{2+} currents, and R-type current that is resistant to all of the above. Of these five components, the L-type component accounts for about 15 % of the total. In the present study, we observed a 2.7-fold increase in the levels of $Ca_V1.2$ L-type Ca^{2+} channel protein in cells from thiamine-deficient cultures. Based on the results of the aforementioned study (Randall and Tsien 1995), such a 2.7-fold increase in the L-type component would result in a 41 % increase in the total HVA Ca^{2+} current. It thus appears that the observed increase in $Ca_V1.2$ protein can explain most, but not all, of the observed increase in HVA Ca^{2+} channel current. The remaining increase in HVA Ca^{2+} channel current may be due to increased expression of other alpha subunits beside $Ca_V1.2$. One caveat to this calculation is that Western blot experiments measured total cellular protein, whereas the electrophysiological recordings detect only functionally channels in the plasma membrane. If a significant fraction of the increased $Ca_V1.2$ protein level does not form functional channels, our calculation will overestimate its role in the alterations observed in cells from thiamine-deficient cultures.

The signaling pathway whereby thiamine deficiency results in increased Ca^{2+} channel protein levels is unknown. Future experiments should explore these pathways and determine if they are conserved in different regions of the brain and neurodegenerative conditions. In a previous study, Randall and Tsien (1995) observed the density of HVA Ca^{2+} channel current in cerebellum granular neurons as a function of time in culture. They reported very low Ca^{2+} currents after 1 day in culture, with a progressive increase until day 5, at which point Ca^{2+} currents stabilized. We observed Ca^{2+} currents at a single time point of 7 days in culture because our previous results indicate that 7 days is sufficient for the in vitro effects of thiamine deficiency to stabilize (Cruz et al. 2012; Oliveira et al. 2007). We thus do not know at which stage during the maturation of the cell culture Ca^{2+} currents in cells from thiamine-deficient cultures begin to differ significantly from control cultures. Possibly, the differences in the pattern of expression of HVA Ca^{2+} channels in cells from thiamine-deficient cultures as compared to control cultures may change at different stages of culture maturation.

Neurodegeneration caused by thiamine deficiency occurs primarily in encephalic areas, especially the cerebellum (Mulholland 2006; Troncoso et al. 1981; Pannunzio et al. 2000; Butterworth 1993). Previous studies have linked thiamine deficiency to Ca^{2+} deregulation in the thalamus (Hazell et al. 1998) and cortical neurons (Lee et al. 2010), however both used a pharmacological approach to develop thiamine deficiency. Here, we describe, for the first time, Ca^{2+} deregulation in cerebellum granular neurons caused by thiamine deficiency, without any pharmacological interference. Ca^{2+} homeostasis is a pivotal process in a cell that appears to be finely tuned by

several systems including an array of voltage gated Ca^{2+} channels and Ca^{2+} buffering mechanisms (Berridge et al. 1999; Berridge et al. 2000; Bootman et al. 2001; Oh et al. 2013; Maravall et al. 2000). Previously, using the same in vitro approach to study ion channels in granule neurons, we reported a decrease in A-type K^+ current caused by thiamine deficiency. In that study, computation modeling predicted an increase in excitability (Cruz et al. 2012). In the current study, computation modeling indicates that the increase in Ca^{2+} current caused by thiamine deficiency does not compensate for the effects of decreased K^+ conductance. Future studies should test the model predictions using recordings in cerebellar brain slices.

Thiamine deficiency is a neurodegenerative condition affecting the energy metabolism. Several neurodegenerative diseases show energy metabolism impairments and Ca^{2+} signaling alterations. This link between energy metabolism and Ca^{2+} homeostasis open a broad field in the search for new targets in neurodegenerative diseases.

Conclusion

In conclusion, thiamine deficiency augments $Ca_V1.2$ protein levels and increases Ca^{2+} current density in cerebellum granular neurons which probably leads to increase in Ca^{2+} entry building up a scenario predisposing to neurodegeneration.

Acknowledgments This study was funded by São Paulo Research Foundation (FAPESP), Project Number 2012/50336-2 to FAO. DCML held a scholarship from Coordination for the Improvement of Higher Education Personnel (CAPES). C. Kushmerick and J.S. Cruz were funded by CNPq (The National Council for Scientific and Technological Development) research fellowships.

Compliance with Ethical Standards

Conflict of interest The authors declare that they have no conflict of interest.

References

Berridge M, Lipp P, Bootman M (1999) Calcium signalling. Curr Biol 9(5):R157–159

Berridge MJ, Lipp P, Bootman MD (2000) The versatility and universality of calcium signalling. Nat Rev Mol Cell Biol 1(1):11–21. doi:10.1038/35036035

Bootman MD, Lipp P, Berridge MJ (2001) The organisation and functions of local Ca(2+) signals. J Cell Sci 114(Pt 12):2213–2222

Butterworth RF (1993) Pathophysiology of cerebellar dysfunction in the Wernicke-Korsakoff syndrome. Can J Neurol Sci 20(Suppl 3):S123–126

Chadderton P, Schaefer AT, Williams SR, Margrie TW (2014) Sensory-evoked synaptic integration in cerebellar and cerebral cortical neurons. Nat Rev Neurosci 15(2):71–83. doi:10.1038/nrn3648

Chornyy S, Parkhomenko J, Chorna N (2007) Thiamine deficiency caused by thiamine antagonists triggers upregulation of apoptosis inducing factor gene expression and leads to caspase 3-mediated apoptosis in neuronally differentiated rat PC-12 cells. Acta Biochim Pol 54(2):315–322

Cruz JS, Kushmerick C, Moreira-Lobo DC, Oliveira FA (2012) Thiamine deficiency in vitro accelerates A-type potassium current inactivation in cerebellar granule neurons. Neuroscience 221:108–114. doi:10.1016/j.neuroscience.2012.06.053

D'Angelo E, Nieus T, Maffei A, Armano S, Rossi P, Taglietti V, Fontana A, Naldi G (2001) Theta-frequency bursting and resonance in cerebellar granule cells: experimental evidence and modeling of a slow k+-dependent mechanism. J Neurosci 21(3):759–770

Davidson RM, Shajenko L, Donta TS (1994) Amyloid beta-peptide (A beta P) potentiates a nimodipine-sensitive L-type barium conductance in N1E-115 neuroblastoma cells. Brain Res 643(1–2):324–327

Day GS, del Campo CM (2014) Wernicke encephalopathy: a medical emergency. CMAJ 186(8):E295. doi:10.1503/cmaj.130091

Galvin R, Bråthen G, Ivashynka A, Hillbom M, Tanasescu R, Leone MA (2010) EFNS guidelines for diagnosis, therapy and prevention of Wernicke encephalopathy. Eur J Neurol 17(12):1408–1418. doi:10.1111/j.1468-1331.2010.03153.x

Gleichmann M, Mattson MP (2011) Neuronal calcium homeostasis and dysregulation. Antioxid Redox Signal 14(7):1261–1273. doi:10.1089/ars.2010.3386

Hamill OP, Marty A, Neher E, Sakmann B, Sigworth FJ (1981) Improved patch-clamp techniques for high-resolution current recording from cells and cell-free membrane patches. Pflug Arch Eur J Phy 391(2):85–100

Hazell AS, Hakim AM, Senterman MK, Hogan MJ (1998) Regional activation of L-type voltage-sensitive calcium channels in experimental thiamine deficiency. J Neurosci Res 52(6):742–749

Hines ML, Carnevale NT (1997) The NEURON simulation environment. Neural Comput 9(6):1179–1209

Kang KD, Majid AS, Kim KA, Kang K, Ahn HR, Nho CW, Jung SH (2010) Sulbutiamine counteracts trophic factor deprivation induced apoptotic cell death in transformed retinal ganglion cells. Neurochem Res 35(11):1828–1839. doi:10.1007/s11064-010-0249-5

Kawamoto EM, Vivar C, Camandola S (2012) Physiology and pathology of calcium signaling in the brain. Front Pharmacol 3:61. doi:10.3389/fphar.2012.00061

Kim S, Rhim H (2011) Effects of amyloid-beta peptides on voltage-gated L-type Ca(V)1.2 and Ca(V)1.3 Ca(2+) channels. Mol Cells 32(3):289–294. doi:10.1007/s10059-011-0075-x

Kim MJ, Chung YH, Joo KM, Oh GT, Kim J, Lee B, Cha CI (2004) Immunohistochemical study of the distribution of neuronal voltage-gated calcium channels in the nNOS knock-out mouse cerebellum. Neurosci Lett 369(1):39–43. doi:10.1016/j.neulet.2004.07.047

Lee S, Yang G, Yong Y, Liu Y, Zhao L, Xu J, Zhang X, Wan Y, Feng C, Fan Z, Liu Y, Luo J, Ke ZJ (2010) ADAR2-dependent RNA editing of GluR2 is involved in thiamine deficiency-induced alteration of calcium dynamics. Mol Neurodegener 5:54. doi:10.1186/1750-1326-5-54

MacManus A, Ramsden M, Murray M, Henderson Z, Pearson HA, Campbell VA (2000) Enhancement of (45)Ca(2+) influx and voltage-dependent Ca(2+) channel activity by beta-amyloid-(1-40) in rat cortical synaptosomes and cultured cortical neurons. Modulation by the proinflammatory cytokine interleukin-1beta. J Biol Chem 275(7):4713–4718

Maravall M, Mainen ZF, Sabatini BL, Svoboda K (2000) Estimating intracellular calcium concentrations and buffering without

wavelength ratioing. Biophys J 78(5):2655–2667. doi:10.1016/S0006-3495(00)76809-3

Mattson MP (2007) Calcium and neurodegeneration. Aging Cell 6(3):337–350. doi:10.1111/j.1474-9726.2007.00275.x

Mulholland PJ (2006) Susceptibility of the cerebellum to thiamine deficiency. Cerebellum 5(1):55–63. doi:10.1080/14734220600551707

Oh MM, Oliveira FA, Disterhoft JF (2010) Learning and aging related changes in intrinsic neuronal excitability. Front Aging Neurosci 2:2. doi:10.3389/neuro.24.002.2010

Oh MM, Oliveira FA, Waters J, Disterhoft JF (2013) Altered calcium metabolism in aging CA1 hippocampal pyramidal neurons. J Neurosci 33(18):7905–7911. doi:10.1523/JNEUROSCI.5457-12.2013

Oliveira FA, Galan DT, Ribeiro AM, Santos Cruz J (2007) Thiamine deficiency during pregnancy leads to cerebellar neuronal death in rat offspring: role of voltage-dependent K+ channels. Brain Res 1134(1):79–86. doi:10.1016/j.brainres.2006.11.064

Pácal L, Kuricová K, Kaňková K (2014) Evidence for altered thiamine metabolism in diabetes: is there a potential to oppose gluco- and lipotoxicity by rational supplementation? World J Diabetes 5(3):288–295. doi:10.4239/wjd.v5.i3.288

Pannunzio P, Hazell AS, Pannunzio M, Rao KV, Butterworth RF (2000) Thiamine deficiency results in metabolic acidosis and energy failure in cerebellar granule cells: an in vitro model for the study of cell death mechanisms in Wernicke's encephalopathy. J Neurosci Res 62(2):286–292

Randall A, Tsien RW (1995) Pharmacological dissection of multiple types of Ca2+ channel currents in rat cerebellar granule neurons. J Neurosci 15(4):2995–3012

Sola E, Prestori F, Rossi P, Taglietti V, D'Angelo E (2004) Increased neurotransmitter release during long-term potentiation at mossy fibre-granule cell synapses in rat cerebellum. J Physiol 557(Pt 3):843–861. doi:10.1113/jphysiol.2003.060285

Szydlowska K, Tymianski M (2010) Calcium, ischemia and excitotoxicity. Cell Calcium 47(2):122–129. doi:10.1016/j.ceca.2010.01.003

Troncoso JC, Johnston MV, Hess KM, Griffin JW, Price DL (1981) Model of Wernicke's encephalopathy. Arch Neurol 38(6):350–354

Tymianski M, Charlton MP, Carlen PL, Tator CH (1993) Source specificity of early calcium neurotoxicity in cultured embryonic spinal neurons. J Neurosci 13(5):2085–2104

Ueda K, Shinohara S, Yagami T, Asakura K, Kawasaki K (1997) Amyloid beta protein potentiates Ca2+ influx through L-type voltage-sensitive Ca2+ channels: a possible involvement of free radicals. J Neurochem 68(1):265–271

Veng LM, Mesches MH, Browning MD (2003) Age-related working memory impairment is correlated with increases in the L-type calcium channel protein alpha1D (Cav1.3) in area CA1 of the hippocampus and both are ameliorated by chronic nimodipine treatment. Brain Res Mol Brain Res 110(2):193–202

Wang X, Wang B, Fan Z, Shi X, Ke ZJ, Luo J (2007) Thiamine deficiency induces endoplasmic reticulum stress in neurons. Neuroscience 144(3):1045–1056. doi:10.1016/j.neuroscience.2006.10.008

Yadav UC, Kalariya NM, Srivastava SK, Ramana KV (2010) Protective role of benfotiamine, a fat-soluble vitamin B1 analogue, in lipopolysaccharide-induced cytotoxic signals in murine macrophages. Free Radic Biol Med 48(10):1423–1434. doi:10.1016/j.freeradbiomed.2010.02.031